

A New Structural Model of Enzymatic Lignin with Multiring Aromatic Clusters

Yupeng Wang, Yucui Hou, He Li, Weize Wu,* Shuhang Ren, and Jianwei Li

Cite This: *ACS Omega* 2022, 7, 18861–18869

Read Online

ACCESS |



Metrics & More

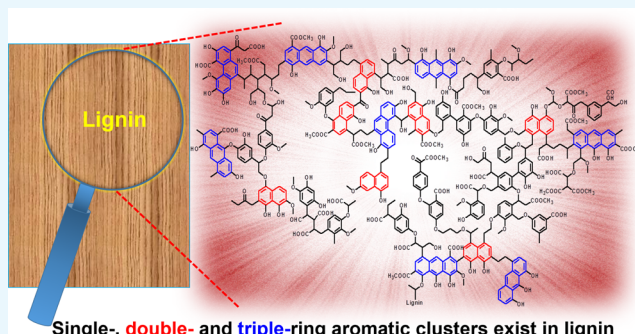


Article Recommendations



Supporting Information

ABSTRACT: Lignin is a natural aromatic compound in plants. Several lignin structural models have been proposed in the past years, but all the models cannot be converted to benzene carboxylic acids (BCAs) for all aromatic rings connected to oxygen. This inspired us to explore the structures of lignin. Based on the yields of BCAs, the results of ^{13}C NMR and ethanolysis residues, and gas chromatography–mass spectrometry and electro-spray ionization mass spectrometry of ethanolysis of lignin, we have constructed a structural model of lignin with a formula $\text{C}_{6407}\text{H}_{6736}\text{O}_{2590}\text{N}_{147}\text{S}_3$. The model not only satisfies the results of analyses, but also explains the generation of BCAs from lignin oxidation and the ethanolysis products. Importantly, double-ring and triple-ring aromatic clusters are found in lignin, and some of them are connected by alkyl bridges, which results in conventional low conversions of lignin. Our findings in the structures of lignin may significantly influence the structures and applications of lignin.

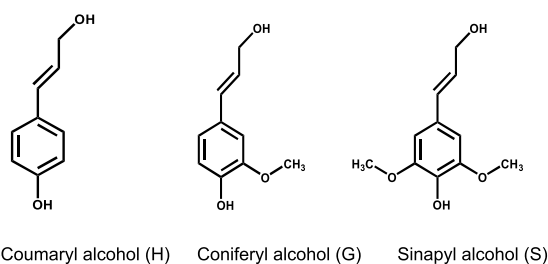


1. INTRODUCTION

Biomass is highly attractive for a sustainable source of chemicals, materials, and fuels.¹ As the most abundant form of biomass, lignocellulose has a production of around 170 billion metric tons per year.² Lignocellulose is inedible for humans, and it is mainly found in agricultural and forestry waste. The efficient use of this cheap and abundant carbon-neutral resource can greatly alleviate the energy crisis and environmental problems. Therefore, lignocellulose is a highly promising alternative to fossil energy sources.

As we know, cellulose, hemicellulose, and lignin are the three main components in lignocellulose. Among them, hemicellulose and cellulose are composed of five-carbon and six-carbon sugars,³ but the structure of lignin is very complicated and there is no exact structural model.⁴ Lignin acts as a binder in lignocellulose and holds cellulose and hemicellulose together.⁵ More specifically, lignin is a three-dimensional reticulated macromolecular structure made up of randomly crosslinked oxygenated aromatic units. By crosslinking with cellulose and hemicellulose, lignin provides strength, rigidity, and flexibility with lignocellulose as well as aiding in water transport and protecting against attack by marauding insects and microorganisms. Nowadays, in human's daily life, the majority of lignin is used for direct combustion for heat and power because of its complicated structure. Only by clarifying the structure of lignin can we put it to better use. Traditionally, as shown in Scheme 1, three phenylpropane structures are considered as basic structural units in lignin.^{4,6–8} The most prominent feature is that the structural units of lignin are all

Scheme 1. Structures of the Primary Building Blocks of Lignin



single-ring aromatic clusters and directly connected with oxygen functional groups, such as $-\text{OH}$ and $-\text{OCH}_3$. Therefore, lignin is attracting much attention because of its potential as a renewable aromatic,^{9,10} especially monophenols.¹¹ However, we produced almost all types of benzene carboxylic acids (BCAs) from enzymatic lignin by alkali-oxygen oxidation in this work. The structures of 12 BCAs are shown in Scheme S1. To the best of our knowledge, the production of BCAs from lignin has not been reported. On the

Received: March 24, 2022

Accepted: May 10, 2022

Published: May 24, 2022



other hand, BCAs cannot be produced from the existing lignin structures (as shown in Scheme 1) for every aromatic ring directly connected with oxygen functional groups. What are the real structural units in lignin leading to BCAs' formation?

The most accredited theories about the lignin structure go back to the early 1960s. Freudenberg performed the process of lignin biosynthesis in plants by coniferyl alcohol¹² and then plotted the first structural model of lignin through detecting the intermediates during lignin synthesis.¹³ Then Nimz proposed another structural model of lignin by detecting the products of thioacetic acid depolymerization of lignin.¹⁴ The above two most famous structural models put a foundation for later research studies about lignin structures and many transformation routes of lignin. After that, several structural models of lignin were further proposed.^{15–17} Recently, several review articles^{18,19} have discussed the structures of lignin, but the features of lignin structures are similar to those previously proposed. In summary, these structural models in the literature are very similar in terms of structure units and chemical bonds, mainly including β -O-4 ether bonds and β -5, β -1, β - β , 5-5 strong carbon bonds; and the structural units are all single-ring aromatic clusters directly connected with $-\text{OH}$ or $-\text{OCH}_3$.

There are two main methods to analyze the lignin structure: direct spectrum characterization and inversion of depolymerization products. As for the spectrum method, solid ^{13}C NMR is an effective tool for characterizing the structures of organic macromolecules. The signal areas are proportional to the amount of carbon contained in each functional group.²⁰ Peak fitting of solid ^{13}C NMR spectra is then used to study the structures in detail. Nowadays, solid ^{13}C NMR plays an important role in the structure characterization of oil shale,²¹ coal,²² and lignin.^{23–29} Hence, the method was also applied in this work to study the structure of lignin.

As for the depolymerization method, to better retrieve lignin's structure, it is expected to find a suitable way to produce the real molecular structure originating from lignin, that is to say, neither over depolymerization nor repolymerization happened. At present, many chemicals are produced from lignin through hydrolysis,³⁰ hydrogenolysis,³¹ and pyrolysis.³² Here, we obtained BCAs through the oxidation of lignin. However, we only make sure that in lignin there exist aromatic rings that are not connected directly with oxygen functional groups. The oxidation method is too harsh to depolymerize lignin to relatively small acids, so we cannot obtain the macromolecular structure in lignin.

Supercritical ethanolysis is an effective way to depolymerize organic substances by breaking weak bonds (such as C–O bonds) without further reactions or called the second reactions. It has been widely used in the depolymerization of lignin.^{33,34} As we know, C–O bonds are the most common linkages in lignin. Hence, we can obtain the macromolecules from lignin through supercritical ethanolysis. After the depolymerization of lignin, the detection of products is also a pivotal factor in deducing the structure of lignin. Gas chromatography–mass spectrometry (GC–MS) is usually used in most cases; however, some strongly polar and/or less volatile products cannot be detected with GC–MS.³⁵ Thus, we applied electrospray ionization mass spectrometry (ESI–MS) to detect ethanolysis products of lignin, which is adapted for the investigation of both the primary and supramolecular structures of biopolymers,³⁶ and it is also suitable to detect solutions containing nonvolatile and thermally labile compounds with high molecular weights.³⁷

As mentioned above, all the proposed structural models and structural units of lignin before cannot be oxidized to BCAs. In this work, we proposed a new lignin structure model based on the distribution of BCAs combined with the results of ultimate analysis, Fourier-transform infrared spectroscopy, ^{13}C NMR, and ethanolsolysis of lignin. The result showed that there were not only single-ring aromatic clusters directly connected to oxygen atoms, but also multiring aromatic clusters, including double-ring aromatic clusters and triple-ring aromatic clusters in lignin.

2. RESULTS AND DISCUSSION

The alkali-oxygen oxidation of the lignin was performed, and the effects of temperature, initial oxygen pressure, reaction time, and the alkali/enzymatic lignin on reaction were investigated. The results are shown in Figures S1–S4 in the Supporting Information (SI). It can be found that 11 kinds of BCAs have been obtained. The distribution of BCAs at the maximum yield is shown in Figure S5 and Table 1. The total

Table 1. Yields of BCAs from Enzymatic Lignin via Oxidation and Their Distribution in the Structural Model

products	mass yield/wt %	molar yield/ $\text{mmol}\cdot\text{g}^{-1}$	distribution in products	distribution in the model
benzoic acid	0.182	1.49×10^{-2}	1.99	2
phthalic acid	0.686	4.13×10^{-2}	4.49	5
isophthalic acid	0.148	0.89×10^{-2}	1.19	1
trimellitic acid	1.14	5.43×10^{-2}	7.24	7
hemimellitic acid	0.488	2.32×10^{-2}	3.09	3
trimesic acid	0.390	1.86×10^{-2}	2.48	2
prehnitic acid	0.191	0.75×10^{-2}	1	1
pyromellitic acid	0.963	3.79×10^{-2}	5.05	5
mellophanic acid	0.967	3.81×10^{-2}	5.08	5
benzene pentacarboxylic acid	2.05	6.88×10^{-2}	9.17	9
mellitic acid	0.937	2.74×10^{-2}	3.65	4

mass yield of BCAs was 8.14% obtained under the optimum conditions. It can be seen that BCAs containing three or more carboxyl groups are main products, especially benzene pentacarboxylic acid. This result is undoubtedly determined by the structure of the lignin.

We constructed the new structural units of the lignin based on BCA distribution, and the data processing of BCAs is shown in Section 1.2 of the SI. The amounts of BCA distribution in the model are also shown in Table 1.

From Table 1, we can obtain the total molecular weight (10,604) of BCAs by adding the number in column 5 of Table 1 multiplied by BCA's molecular weight. Because the maximum yield of BCAs is 8.14%, so the molecular weight of the lignin structure model can be roughly calculated as $10,604/0.0814 = 130,270$ Da (a hypothetical value proposed to construct the lignin model to ensure that the lowest-BCA, isophthalic acid, has one aromatic structural unit). Then, based on the ultimate analysis of the lignin (shown in Table 2), the atom numbers of C, H, O, N, and S were calculated as 6404, 7035, 2763, 147, and 3, respectively, in the structural model.

CP/MAS ^{13}C NMR was utilized to analyze the lignin to obtain structural parameters of various carbons. The ^{13}C NMR spectrum and peak fitting spectra of enzymatic lignin are

Table 2. Proximate and Ultimate Analyses of Enzymatic Lignin^a

proximate analysis (wt %)			ultimate analysis (in daf. Basis, wt %)				
<i>M</i> _{ad}	<i>A</i> _{ad}	<i>V</i> _{daf}	C	H	O ^b	N	S
8.31	1.84	61.29	58.99	5.41	33.94	1.58	0.08

^aad: air-dry basis; d: dry basis; daf: dry-and-ash-free basis. *M*: moisture; *A*: ash; *V*: volatile matter content. ^bBy difference.

shown in Figure S6, and every position of carbon is shown in Table S1.

Based on the peak fitting spectra of ¹³C NMR, carbon types and molar content have been determined and are shown in Table 3. The specified carbon numbers in the structural model are shown in column 6 of Table 3.

Based on the data in Table 3, several structure parameters of the lignin were calculated as follows.

- (1) Ratio of aromatic carbon (f_a): $f_a = f_{ar}^H + f_{ar}^B + f_{ar}^C + f_{ar}^{O1} + f_{ar}^{O2} = 55.3\%$
- (2) Molar fraction of aromatic bridgehead carbon (X_b): $X_b = f_{ar}^B/f_a = 0.160$
- (3) Ratio of aliphatic carbon (f_{al}): $f_{al} = f_{al}^1 + f_{al}^2 + f_{al}^3 + f_{al}^4 + f_{al}^{O1} + f_{al}^{O2} + f_{al}^{O3} = 35.3\%$
- (4) Substituted degree of aromatic ring (δ): $\delta = (f_{ar}^C + f_{ar}^{O1} + f_{ar}^{O2})/f_a = 0.56$

As a natural aromatic substance, the ratio of aromatic carbon is as high as 55.3%. The substituted degree of aromatic ring (δ) is 0.56, which indicates that more than half aromatic carbons are substituted. The molar fraction of aromatic bridgehead carbon (X_b) is 0.160, which means that there are double- or more ring aromatic clusters in the lignin. The molar fraction of aromatic bridgehead carbon X_b is always an index for multiring aromatic clusters, and the X_b of single-ring, double-ring, and triple-ring aromatic clusters is 0, 0.2, and 0.286, respectively.

To identify a more exact number of aromatic rings, we applied supercritical ethanolsis to break weak bonds (β -O-4 and α -O-4) and obtained liquid products in ethanol. The effects of temperature and reaction time on the yield of ethanolsis products were investigated. The results are shown in Figures S7 and S8. The results of the two figures indicate that the carbon yield of ethanolsis products reaches 54.65% under relatively mild conditions (290 °C, 120 min). The ethanolsis liquid and residue were characterized separately, and it is found that the aromatic bridge carbon of residues over 300 °C is more than that of raw lignin, which may indicate repolymerization. Thus, the ethanolsis liquid and residue obtained at 290 °C were investigated. The total ion chromatogram spectrum obtained using GC-MS is shown in Figure S9, and the compounds identified by the NIST11 database are shown in Table S2. It should be noted that the substances with relative contents higher than 0.5% are considered.

However, only single-ring aromatic clusters were detected by GC-MS; all these structural units conform neither to X_b from ¹³C NMR nor to produce 11 BCAs via oxidation. As mentioned above, because of the limitation of GC-MS, some large-molecule compounds may not be detected, which may result from the residue in the column of GC. Hence, we applied ESI-MS to detect if there were multiring aromatic clusters existing in lignin ethanolsis products. The ESI-MS spectrum is shown in Figure 1.

As shown in Figure 1, the m/z peaks of ethanolsis products focus on 100 to 400, which indicates that the relative molecular mass focuses on 100 to 400. The relative molecular mass is larger than that detected by GC-MS. We could find that single-ring aromatic compounds detected by GC-MS were also detected by ESI-MS as shown in Table S2. In addition, several bigger compound formulas were detected based on the error and isotope analysis, and we could speculate the structures of different aromatic ring clusters based on these formulas. The molecular formulas and intensity are shown in Table S3, which includes double-ring and triple-ring aromatics. Then we depicted the structures of these multiring aromatic clusters as shown in Scheme S2. There may be other multiring aromatic cluster isomers based on the formulas, and we just provided ones of the possible structures, which are double- and triple-ring aromatic clusters. The results demonstrate that there exist double-ring and triple-ring aromatic clusters in the lignin.

The ethanolsis residue was also characterized through ¹³C NMR (Figure S10) and Fourier-transform infrared (FTIR) spectroscopy (Figure 2). The ¹³C NMR data were processed using the same way as that of the enzymatic lignin. The total carbon atoms of the structural model are 6404, so the amount of carbon atoms in the ethanolsis residue in the structural model is 2904 for the 54.65% carbon yield of liquid products. The peak fitting of spectrum and the amount of different carbon are shown in Figure S10 and Table 3. We also obtained the structure parameters of the residue as follows.

- (5) Ratio of aromatic carbon (f_a): $f_a = f_{ar}^H + f_{ar}^B + f_{ar}^C + f_{ar}^{O1} + f_{ar}^{O2} = 66.9\%$
- (6) Molar fraction of aromatic bridgehead carbon (X_b): $X_b = f_{ar}^B/f_a = 0.252$
- (7) Ratio of aliphatic carbon (f_{al}): $f_{al} = f_{al}^1 + f_{al}^2 + f_{al}^3 + f_{al}^4 + f_{al}^{O1} + f_{al}^{O2} + f_{al}^{O3} = 30.46\%$
- (8) Substituted degree of aromatic ring (δ): $\delta = (f_{ar}^C + f_{ar}^{O1} + f_{ar}^{O2})/f_a = 0.55$

The substituted degree of aromatic ring (δ) is almost the same as that of the lignin, which means more substitution groups in the ethanolsis residue, considering that multiring aromatic clusters have fewer aromatic carbons that can be substituted. X_b is 0.252, which indicates that double-ring aromatic clusters and triple-ring aromatic clusters exist in the ethanolsis residue at least. During ethanolsis depolymerization, owing to the weak bonds (C-O) being broken, some single- and multi-ring aromatic clusters were extracted into the liquid solution (as shown in Table S2 and Scheme S2), which indicates that some multiring aromatic clusters are also connected with C-O bonds. From the NMR result of ethanolsis residue and liquid products of lignin, we concluded that most multiring aromatic clusters were connected with strong C-C bonds and could not be broken during the ethanolsis process. The numbers of carbon atoms of origin lignin and the ethanolsis residue are compared in Table 3.

From Table 3, the number of oxygen-attached aliphatic carbon decreases notably, which indicates that the most connection manners (β -O-4) in lignin are broken to form phenols and then dissolve in the ethanol solution. In addition, most of the aromatic bridgehead carbon is left in the residue, and a small portion is extracted to liquid products. The mechanism of lignin ethanolsis is shown in Scheme 2 based on lignin alcoholysis results reported in the literature.^{38,39}

The FTIR spectra of the lignin and the ethanolsis residue are shown in Figure 2. In the comparison of these two FTIR

Table 3. Different Types of Carbon between Origin Lignin and Ethanolysis Residues

Carbon type	Symbol	Position	Carbon molar content/%		Carbon number	
			Origin lignin	Ethanolysis residue	Origin lignin	Ethanolysis residue
Aliphatic CH ₃	f_{al}^1	—CH ₃	2.11	3.29	135	96
Aromatic CH ₃	f_{ar}^2		2.87	5.54	184	161
Methylene	f_{al}^3		5.36	5.40	343	157
Branched central carbon	f_{al}^4		6.66	5.14	427	149
Oxygen-attached aliphatic carbon	f_{al}^{O1}		8.77	8.94	562	260
						
	f_{al}^{O2}		3.32	4.02	213	117
						
	f_{al}^{O3}		6.21	0	398	0
Aromatic protonated carbon	f_{ar}^H		15.38	13.26	985	385
						
						
Aromatic bridgehead carbon	f_{ar}^B		8.83	16.36	565	475
Alkyl-substituted carbon	f_{ar}^C		15.37	16.96	984	493
Oxygen-attached aromatic carbon	f_{ar}^{O1}		7.69	9.97	492	290
						
						
Carboxyl carbon	f_a^C	—COOR	3.51	1.86	225	54
		—COOH	3.71	0.72	238	21
Carbonyl carbon	f_a^O		2.13	0	136	0

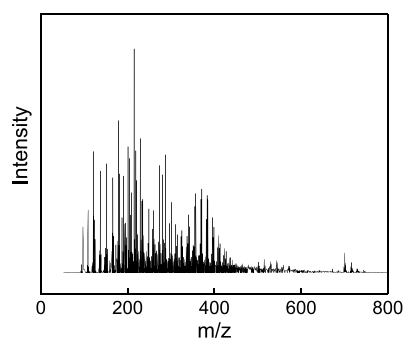


Figure 1. Negative-mode ESI-MS spectrum of ethanolysis products.

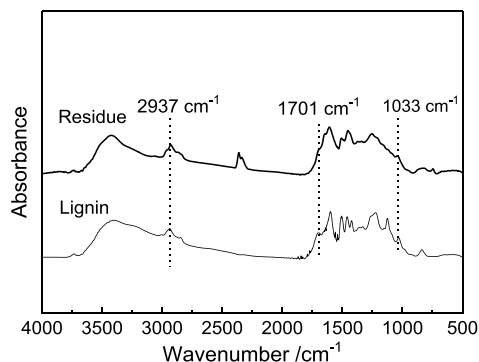
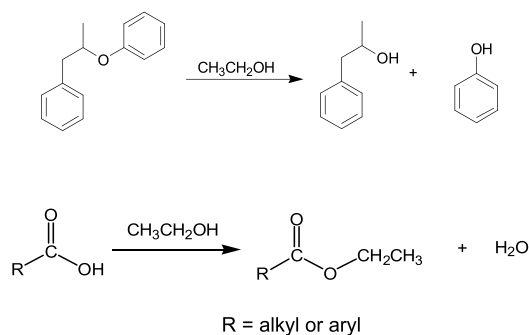


Figure 2. FTIR spectra of enzymatic lignin and ethanolysis residue.

Scheme 2. Possible Mechanisms during Ethanolysis



spectra, the intensity of the associative hydroxyl peak becomes narrow at $3500\text{--}3300\text{ cm}^{-1}$, which can be attributed to some aromatics containing phenolic groups extracted to supercritical ethanol; the intensity of the methyl group peak increases slightly at 2937 cm^{-1} for esterification; the carbonyl groups at 1701 cm^{-1} also decrease after ethanolysis; the C–O–C asymmetric stretching vibration of the ether group decreased at 1127 cm^{-1} after ethanolysis, which indicates the break of ether bonds (β -O-4) during the ethanolysis process.

The amounts of total carbon, aromatic carbon, and bridgehead carbon are shown in Table 4. Based on the result of ESI-MS, we detected large molecules and classified them into single-, double-, and triple-aromatic clusters. Based on elemental analysis and ^{13}C NMR spectra, there are 565, 490, and 75 bridgehead carbon atoms of the structural model of the lignin, ethanolysis residue, and ethanolysis liquid product, respectively. The X_b (0.252) of the ethanolysis residue indicates that the average number of aromatic rings is between two and three. This suggested that almost single rings were extracted and the ethanolysis residue contained only double

Table 4. Distribution of Carbon in the Raw Material, Liquid Products, and Residue

carbon type	enzymatic lignin	ethanolysis liquid product	ethanolysis residue
total carbon number	6404	3500	2904
aromatic carbon number	3543	1600	1943
bridgehead carbon number	565	75	490

and triple-aromatic clusters. Thus, it can be concluded that the ratio of double-ring aromatic clusters: triple-ring aromatic clusters in the ethanolysis residue of lignin is 1:1.09 based on the X_b of the ethanolysis residue. Hence, it can be calculated that the number of the double-ring aromatic clusters is 77, and that of the triple-ring aromatic clusters is 84. According to 75 atoms of bridgehead carbon in the liquid product, the numbers of double- and triple-ring aromatic clusters could be identified as 12 and 13 based on the 1:1.09 ratio of double-ring aromatic clusters to triple-ring aromatic clusters. Meanwhile, we could calculate the number of single-ring aromatic clusters in the liquid product as 216 $((1600 - 12 \times 10 - 13 \times 14)/6 = 216)$.

Based on the calculation of liquid products and ethanolysis residues, there are 216 single-ring aromatic clusters, 89 double-ring aromatic clusters, and 97 triple-ring aromatic clusters in the structural model of the lignin. Thus, the number of all aromatic carbons is adjusted as 3544 $(216 \times 6 + 89 \times 10 + 97 \times 14 = 3544)$.

Based on the yield distribution of BCAs, 44 units in enzymatic lignin can be converted into BCAs during the oxidation process, which indicates that some multiring aromatic clusters cannot be converted into BCAs for their every aromatic ring connected with oxygen. Based on the analysis of the ethanolysis liquid and residue, the multiring aromatic clusters are connected by strong C–C mostly, which causes most of them to be left in the ethanolysis residue, while C–O accounts for a large percentage in the connections of single-ring aromatic clusters.

In addition to C, H, and O, there are N (1.58%) and S (0.08%) elements that exist in the lignin sample based on ultimate analysis (Table 2). X-ray photoelectron spectroscopy (XPS) has been applied to characterize the surface composition of coals^{22,40} and biomass.^{41,42} Here, the S content is too little to be detected by XPS, and the lignin model only contains three S atoms. We applied XPS to characterize the valence and form of N in the lignin sample. As displayed in Figure 3 and Table 5, the XPS N 1s spectrum of the lignin

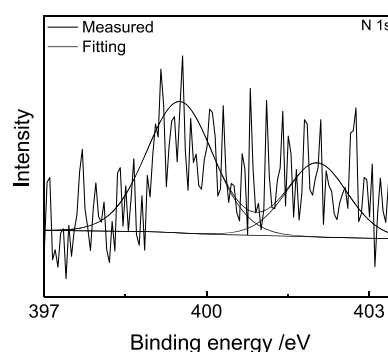


Figure 3. XPS spectrum (N 1s) of enzymatic lignin and their fitting curves.

Table 5. Distribution of Carbon in the Raw Material, Liquid Product, and Residue

elemental peak	functionality	binding energy/ eV	mole content/%
N 1s	amino	399.50	66.0
	chemisorbed nitrogen oxides	402.04	34.0

sample is fitted with two peaks at 399.50 and 402.04 eV, corresponding to amino and chemisorbed nitrogen oxides, respectively. Based on the area of two peaks and the result of ultimate analysis, the numbers of amino and chemisorbed nitrogen oxides are found to be 97 and 50. The amino form of nitrogen may result from amino acids and proteins.⁴² In addition, as the source of lignin we used, corn cob contains 17 amino acids besides cellulose, hemicellulose, and lignin.⁴³ The trace S may also result from the methionine that exist in the corn cob.

Based on the above information, we constructed a structural model of the enzymatic lignin (as shown in Figure 4) with a formula $C_{6407}H_{6736}O_{2590}N_{147}S_3$. In the structural model, there are 44 aromatic units in red, which can be converted to BCAs via alkali-oxygen oxidation. In addition, the detected aromatic units by GC/MS and ESI/MS were depicted, while they are connected with C–O bonds. Many multiring aromatic clusters are connected with C–C bonds. In Table S4, the results of the structural model are compared with those from experiments of lignin, and it can be found that the average absolute relative deviation is 1.4%. The formation of BCAs and the ethanolysis result can be reflected in the constructed model of lignin.

The structural model presented in this work has the following uses. First, multiring aromatic clusters and their connections with C–C bonds can explain the low conversions of lignin to aromatic compounds. Second, the model provides information that more valuable aromatic chemicals like naphthene- and anthanthrene-based compounds can be obtained potentially from lignin. In the future experiments, it is necessary to consider to cleavage C–C bonds between aromatic clusters during the depolymerization of lignin and then yield aromatic chemicals. Third, it is necessary to consider the formation mechanism and functions of lignin in plants according to the new model because there are multiring aromatic clusters in lignin. Fourth, the findings of multiring aromatic clusters could be helpful for computational analyses, such as new model construction and parameter optimization.

3. CONCLUSIONS

In summary, we constructed a new model molecular formula of enzymatic lignin with a molecular formula of $C_{6407}H_{6736}O_{2590}N_{147}S_3$ and a model molecular weight of 127,214 Da. The structural model of lignin includes single-ring, double-ring, and triple-ring clusters. In addition, only a small part of aromatic clusters where at least one benzene ring is not directly connected with oxygen can be oxidized to BCAs. Most single-ring clusters are connected with weak C–O bonds, while most multiring aromatic clusters are connected with C–C bonds. The model could reflect not only the yield of BCAs, but also the products of ethanolysis and the ^{13}C NMR result of enzymatic lignin.

4. MATERIALS AND METHODS

4.1. Materials. Enzymatic lignin used in this work was purchased from Shandong Longlive Bio-technology Co., Ltd., Shandong province, China. The isolated process of enzymatic lignin is depicted as reported elsewhere.⁷ Briefly, corncob was used to isolate lignin via enzymatic hydrolysis. First, corncob was treated with dilute acid to remove hemicellulose and then treated with cellulase to remove cellulose. After that, the residue was dissolved in an alkaline solution and then precipitated by adjusting its pH, and the residue from precipitation is enzymatic lignin. It was pulverized to pass through a 200-mesh sieve (particle sizes less than 0.075 mm) before use.

The proximate and ultimate analyses of enzymatic lignin were conducted, and the results are listed in Table 2. Sodium hydroxide (96%), concentrated sulfuric acid (98%), ethanol ($\geq 99.7\%$), and phosphoric acid ($\geq 85\%$) were purchased from Beijing Chemical Plant, Beijing, China; All reagents are analytical reagents. Acetonitrile (99.9%, HPLC) was purchased from Thermo Fisher Scientific Co., Ltd., Shanghai, China; oxygen (99.995%) and nitrogen (99.9%) were supplied by Beijing Beiweng Gas Industry Co., Ltd., Beijing, China.

4.2. Analyses of Enzymatic Lignin and Ethanolysis Residues. Based on the ion-exchange method (Section 1.3 in the Supporting Information),⁴⁴ the amount of the phenolic group and carboxyl group were determined. The results are shown in Table 6.

Structural parameters of various carbons in enzymatic lignin and ethanolysis residues were obtained by ^{13}C NMR. All CP/MAS ^{13}C NMR spectra were obtained on a Bruker AV-300 spectrometer with a ^{13}C frequency of 67.8 MHz. The chemical shift of ^{13}C was calibrated by adamantane (an external standard substance). The cross-polarization contact time was 2 ms, and the cycle time was 7 s.

FTIR spectra of enzymatic lignin and ethanolysis were recorded on a Nicolet 6700 FTIR spectrometer at a resolution of 4 cm^{-1} in reflectance mode with a measuring region of $4000\text{--}400\text{ cm}^{-1}$. Samples for the FTIR measurement were prepared by mixing 1 mg of sample with 100 mg of KBr, and the mixture was pressed to form a pellet.

XPS analysis of enzymatic lignin was conducted on an X-ray photoelectron spectroscope (Thermo Fisher ESCALAB-250) equipped with a monochromatized Al K α X-ray source and operated at 150 W. The pass energies of whole spectra and narrow ones of all elements were fixed at 200 and 30 eV, respectively. Energy calibration was made using the containment carbon (C 1s = 284.6 eV).

4.3. Alkali-Oxygen Oxidation of Enzymatic Lignin.

The oxidation of the enzymatic lignin sample was shown as follows: 1.00 g enzymatic lignin, 0–5 g sodium hydroxide, and 20 mL deionized water were added into a 50 mL high-pressure reactor provided by Hai'an Petroleum Scientific Research Co. Ltd., Jiangsu, China. Before reaction, the reactor was purged by high-purity oxygen and then filled with oxygen to a desired pressure (4–6 MPa). Next, the reactor was heated at a rate of $8\text{--}10\text{ }^\circ\text{C}/\text{min}$ to a desired temperature ($240\text{--}280\text{ }^\circ\text{C}$). When the reaction was finished, the reactor was rapidly cooled to room temperature in an ice-water bath prepared in advance. After releasing the gas, the reaction mixture was filtered, and the pH of the filtrate was adjusted using concentrated sulfuric acid to 1.5. The filtrate was diluted and then analyzed via high-



Figure 4. Proposed structural model of organic matter of enzymatic lignin. Aromatics clusters in red are convertible to BCAs via oxidation.

performance liquid chromatography. Product analysis is provided in the [Supporting Information](#).

4.4. Supercritical Ethanolysis of Enzymatic Lignin and Product Analysis. One gram of lignin and 30 mL ethanol were loaded into a 50 mL high-pressure batch reaction

Table 6. Amount of the Phenolic Group and Carboxyl Group in the Enzymatic Lignin

name	phenolic group	carboxyl group
content/mmol g ⁻¹	3.41	1.65

vessel provided by Hai'an Petroleum Scientific Research Co. Ltd., Jiangsu, China. Before reaction, the reactor was purged with high-purity nitrogen five times. The sealed reactor was then heated to a desired temperature and kept for a desired reaction time. After reaction, the reactor was rapidly cooled to room temperature in an ice-water bath. After releasing the gas, the reaction mixture and reaction vessel were washed with ethanol and then filtered. The ethanolysis products, which were ethanol-soluble fraction (ES), were concentrated by reduced pressure rotary evaporation. The remaining residues were dried at 80 °C in a vacuum oven for 24 h. The conversion of lignin was calculated using eq 1.

$$\text{Conversion} = \left(\frac{m_{\text{lignin}} - m_{\text{residue}}}{m_{\text{lignin}}} \right) \times 100\% \quad (1)$$

The liquid products were detected using an Agilent 7890B-5977A (GC–MS) system equipped with a HP-5 capillary column (30.0 m × 250 μm × 0.25 μm). The injection volume was 1 μL, and the injection split ratio was 20:1. The oven temperature was set to 60 °C and hold for 3 min, then heated to 290 °C and hold for 2 min. Compounds were identified by comparing mass spectra with NIST11 library data. Because some strongly polar or less volatile products cannot be detected with GC–MS, we applied a Bruker micrOTOF-QII for the ESI-TOF-MS test. ESI conditions were 3.5 kV voltage, a dry gas (N₂) flow of 4 L/min, and a dry temperature of 180 °C. All liquid products were tested in negative mode, and the flow rate was 180 μL/h.

■ ASSOCIATED CONTENT

SI Supporting Information

The Supporting Information is available free of charge at <https://pubs.acs.org/doi/10.1021/acsomega.2c01812>.

Detailed information on the alkali-oxidation and supercritical ethanolysis; statistical analysis and supporting graphs of the results (PDF)

■ AUTHOR INFORMATION

Corresponding Author

Weize Wu – State Key Laboratory of Chemical Resource Engineering, Beijing University of Chemical Technology, Beijing 100029, China; orcid.org/0000-0002-0843-3359; Email: wzwu@mail.buct.edu.cn

Authors

Yupeng Wang – State Key Laboratory of Chemical Resource Engineering, Beijing University of Chemical Technology, Beijing 100029, China

Yucui Hou – Department of Chemistry, Taiyuan Normal University, Jinzhong, Shanxi 030619, China; orcid.org/0000-0002-9069-440X

He Li – State Key Laboratory of Chemical Resource Engineering, Beijing University of Chemical Technology, Beijing 100029, China

Shuhang Ren – State Key Laboratory of Chemical Resource Engineering, Beijing University of Chemical Technology, Beijing 100029, China; orcid.org/0000-0003-3253-8852

Jianwei Li – State Key Laboratory of Chemical Resource Engineering, Beijing University of Chemical Technology, Beijing 100029, China; orcid.org/0000-0002-1722-1251

Complete contact information is available at:

<https://pubs.acs.org/10.1021/acsomega.2c01812>

Funding

The project was supported financially by the National Natural Science Foundation of China (No. 22178017 and 21776199).

Notes

The authors declare no competing financial interest.

■ ACKNOWLEDGMENTS

We thank Professors Martyn Poliakoff, Zhenyu Liu, and Qingya Liu for helpful discussions. We also thank the Long-Term Subsidy Mechanism from the Ministry of Finance and the Ministry of Education of PRC (BUCT) for experimental help.

■ REFERENCES

- Ragauskas, A. J.; Williams, C. K.; Davison, B. H.; Britovsek, G.; Cairney, J.; Eckert, C. A.; Frederick, W. J.; Hallett, J. P.; Leak, D. J.; Liotta, C. L. The path forward for biofuels and biomaterials. *Science* **2006**, *311*, 484–489.
- Amidon, T. E.; Liu, S. Water-based woody biorefinery. *Biotechnol. Adv.* **2009**, *27*, 542–550.
- Carpenter, D.; Westover, T. L.; Czernik, S.; Jablonski, W. Biomassfeedstocks for renewable fuel production: A review of the impacts of feedstock and pretreatment on the yield and product distribution of fast pyrolysis bio-oils and vapors. *Green Chem.* **2014**, *16*, 384–406.
- Upton, B. M.; Kasko, A. M. Strategies for the conversion of lignin to high-value polymeric materials: Review and perspective. *Chem. Rev.* **2015**, *116*, 2275–2306.
- Sudarsanam, P.; Ruijten, D.; Liao, Y.; Renders, T.; Koelewijn, S. F.; Sels, B. F. Towards lignin-derived chemicals using atom-efficient catalytic routes. *Trends Chem.* **2020**, *2*, 898–913.
- Li, C.; Zhao, X.; Wang, A.; Huber, G. W.; Zhang, T. Catalytic transformation of lignin for the production of chemicals and fuels. *Chem. Rev.* **2015**, *115*, 11559–11624.
- Wang, Y.; Hou, Y.; Wu, W.; Li, H.; Ren, S.; Li, J. Polycyclic aromatics observed in enzymatic lignin by spectral characterization and ruthenium ion-catalyzed oxidation. *J. Agr. Food Chem.* **2021**, *69*, 12148–12155.
- Wu, K.; Cao, M.; Zeng, Q.; Li, X. Radical and (photo)electron transfer induced mechanisms for lignin photo- and electro-catalytic depolymerization. *Green Energy Environ.* **2022**, DOI: [10.1016/j.gee.2022.02.011](https://doi.org/10.1016/j.gee.2022.02.011).
- Constant, S.; Wienk, H. L. J.; Frissen, A. E.; Peinder, P. D.; Boelens, R.; Es, D. S. V.; Grisel, R. J. H.; Weckhuysen, B. M.; Huijgen, W. J. J.; Gosselink, R. J. A. New insights into the structure and composition of technical lignins: A comparative characterisation study. *Green Chem.* **2016**, *18*, 2651–2665.
- Wang, X.; Feng, S.; Wang, Y.; Zhao, Y.; Huang, S.; Wang, S.; Ma, X. Enhanced hydrodeoxygenation of lignin-derived anisole to arenes catalyzed by Mn-doped Cu/Al₂O₃. *Green Energy Environ.* **2022**, DOI: [10.1016/j.gee.2021.12.004](https://doi.org/10.1016/j.gee.2021.12.004).
- Hu, J.; Shen, D.; Rui, X.; Wu, S.; Zhang, H. Free-radical analysis on thermochemical transformation of lignin to phenolic compounds. *Int. J. Remote Sens.* **2012**, *27*, 285–293.
- Freudenberg, K. Biosynthesis and constitution of lignin. *Nature* **1959**, *183*, 1152–1155.

- (13) Freudenberg, K. Lignin: Its constitution and formation from p-hydroxycinnamyl alcohols: Lignin is duplicated by dehydrogenation of these alcohols; intermediates explain formation and structure. *Science* **1965**, *148*, 595–600.
- (14) Nimz, D. H. Beech lignin — Proposal of a constitutional scheme. *Angew. Chem., Int. Ed.* **1974**, *13*, 313–321.
- (15) Adler, E. Lignin chemistry—Past, present and future. *Wood Sci. Technol.* **1977**, *11*, 169–218.
- (16) Glasser, W. G.; Glasser, H. R. Simulation of reactions with lignin by computer (simrel). II. A model for softwood lignin. *Holzforchung* **1974**, *28*, 5–11.
- (17) Sakakibara, A. A structural model of softwood lignin. *Wood Sci. Technol.* **1980**, *14*, 89–100.
- (18) Ralph, J.; Lapierre, C.; Boerjan, W. Lignin structure and its engineering. *Curr. Opin. Biotechnol.* **2019**, *56*, 240–249.
- (19) Sun, R. Lignin source and structural characterization. *ChemSusChem* **2020**, *13*, 4385–4393.
- (20) Leary, G. J.; Newman, R. H. *Cross polarization/magic angle spinning nuclear magnetic resonance (CP/MAS NMR) spectroscopy*; Lin, S. Y., Dence, C. W., Eds.; Springer: Berlin, Heidelberg, 1992; pp 146–161.
- (21) Tong, J.; Han, X.; Wang, S.; Jiang, X. Evaluation of structural characteristics of Huadian oil shale kerogen using direct techniques (solid-state ^{13}C NMR, XPS, FT-IR, and XRD). *Energy Fuels* **2011**, *25*, 4006–4013.
- (22) Li, Z.; Wei, X.; Yan, H.; Zong, Z. Insight into the structural features of Zhaotong lignite using multiple techniques. *Fuel* **2015**, *153*, 176–182.
- (23) Kang, X.; Kirui, A.; Dickwella Widanage, M. C.; Mentink-Vigier, F.; Cosgrove, D. J.; Wang, T. Lignin-polysaccharide interactions in plant secondary cell walls revealed by solid-state NMR. *Nat. Commun.* **2019**, *10*, 347.
- (24) Fu, L.; McCallum, S. A.; Miao, J.; Hart, C.; Tudryn, G. J.; Zhang, F.; Linhardt, R. J. Rapid and accurate determination of the lignin content of lignocellulosic biomass by solid-state NMR. *Fuel* **2015**, *141*, 39–45.
- (25) Mao, J.; Holtman, K. M.; Scott, J. T.; Kadla, J. F.; Schmidt-Rohr, K. Differences between lignin in unprocessed wood, milled wood, mutant wood, and extracted lignin detected by ^{13}C solid-state NMR. *J. Agr. Food Chem.* **2006**, *54*, 9677–9686.
- (26) Hawkes, G. E.; Smith, C. Z.; Utley, J. H. P.; Vargas, R. R.; Viertler, H. A comparison of solution and solid state ^{13}C NMR spectra of lignins and lignin model compounds. *Holzforchung* **1993**, *47*, 302–312.
- (27) Terashima, N.; Atalla, R. H.; Vanderhart, D. L. Solid state NMR spectroscopy of specifically ^{13}C -enriched lignin in wheat straw from coniferin. *Phytochemistry* **1997**, *46*, 863–870.
- (28) Evstigneyev, E. I.; Mazur, A. S.; Kalugina, A. V.; Pranovich, A. V.; Vasilyev, A. V. Solid-state ^{13}C CP/MAS NMR for alkyl-o-aryl bond determination in lignin preparations. *J. Wood Chem. Technol.* **2018**, *38*, 137–148.
- (29) Aoki, D.; Nomura, K.; Hashiura, M.; Imamura, Y.; Miyata, S.; Terashima, N.; Matsushita, Y.; Nishimura, H.; Watanabe, T.; Katahira, M.; Fukushima, K. Evaluation of ring-5 structures of guaiacyl lignin in ginkgo biloba L. Using solid- and liquid-state ^{13}C NMR difference spectroscopy. *Holzforchung* **2019**, *73*, 1083–1092.
- (30) Deuss, P. J.; Scott, M.; Tran, F.; Westwood, N. J.; de Vries, J. G.; Barta, K. Aromatic monomers by in situ conversion of reactive intermediates in the acid-catalyzed depolymerization of lignin. *J. Am. Chem. Soc.* **2015**, *137*, 7456–7467.
- (31) Yan, N.; Zhao, C.; Dyson, P. J.; Wang, C.; Liu, L. T.; Kou, Y. Selective degradation of wood lignin over noble-metal catalysts in a two-step process. *ChemSusChem* **2008**, *1*, 626–629.
- (32) Mohan, D.; Pittman, C. U., Jr.; Steele, P. H. Pyrolysis of wood/biomass for bio-oil: A critical review. *Energy Fuels* **2006**, *20*, 848–889.
- (33) Huang, X.; Korányi, T. I.; Boot, M. D.; Hensen, E. J. M. Ethanol as capping agent and formaldehyde scavenger for efficient depolymerization of lignin to aromatics. *Green Chem.* **2015**, *17*, 4941–4950.
- (34) Kouris, P. D.; van Osch, D. J. G. P.; Cremers, G. J. W.; Boot, M. D.; Hensen, E. J. M. Mild thermolytic solvolysis of technical lignins in polar organic solvents to a crude lignin oil. *Sustainable Energy Fuels* **2020**, *4*, 6212–6226.
- (35) Liu, F.; Wei, X.; Xie, R.; Wang, Y.; Li, W.; Li, Z.; Li, P.; Zong, Z. Characterization of oxygen-containing species in methanolysis products of the extraction residue from Xianfeng lignite with negative-ion electrospray ionization fourier transform ion cyclotron resonance mass spectrometry. *Energy Fuels* **2014**, *28*, 5596–5605.
- (36) Evtuguin, D. V.; Amado, F. M. L. Application of electrospray ionization mass spectrometry to the elucidation of the primary structure of lignin. *Macromol. Biosci.* **2003**, *3*, 339–343.
- (37) Evtuguin, D. V.; Domingues, P.; Amado, F. L.; Pascoal Neto, C.; Ferrer Correia, A. J. Electrospray ionization mass spectrometry as a tool for lignins molecular weight and structural characterisation. *Holzforchung* **1999**, *53*, 525–528.
- (38) Singh, S. K.; Nandeshwar, K.; Ekhe, J. D. Thermochemical lignin depolymerization and conversion to aromatics in subcritical methanol: Effects of catalytic conditions. *New J. Chem.* **2016**, *40*, 3677–3685.
- (39) Song, Q.; Wang, F.; Cai, J.; Wang, Y.; Zhang, J.; Yu, W.; Xu, J. Lignin depolymerization (LDP) in alcohol over nickel-based catalysts via a fragmentation–hydrogenolysis process. *Energy Environ. Sci.* **2013**, *6*, 994–1007.
- (40) Wang, Y.; Wei, X.; Xie, R.; Liu, F.; Li, P.; Zong, Z. Structural characterization of typical organic species in Jincheng No. 15 anthracite. *Energy Fuels* **2015**, *29*, 595–601.
- (41) Bañuls-Ciscar, J.; Abel, M. L.; Watts, J. F. Characterisation of cellulose and hardwood organosolv lignin reference materials by XPS. *Surf. Sci. Spectra* **2016**, *23*, 1–8.
- (42) Shchukarev, A.; Sundberg, B.; Mellerowicz, E.; Persson, P. XPS study of living tree. *Surf. Interface Anal.* **2002**, *34*, 284–288.
- (43) Chen, J.; Yu, W.; Yu, R.; Wu, H.; Wu, D.; Lai, F. Analysis of the nutritional components of corn cobs. *Modern Food Sci. Technol.* **2012**, *28*, 1073–1075.
- (44) Zhou, J.; Wang, Y.; Huang, X.; Zhang, S.; Lin, X. Determination of o-containing functional groups distribution in low-rank coals by chemical titration. *J. Fuel Chem. Technol.* **2013**, *41*, 134–138.